FULL PAPER

First Principles Calculations of Charge Transfer Excitations in Polymer–Fullerene Complexes: Influence of Excess Energy

*Dorota Niedzialek, Ivan Duchemin, Thiago Branquinho de Queiroz, Silvio Osella, Akshay Rao, Richard Friend, Xavier Blase, Stephan Kümmel, and David Beljonne**

The ability of quantum simulations to predict the electronic structure at donor/acceptor interfaces and correlate it with the quantum efficiency of organic solar cells remains a major challenge. The need to describe with increased accuracy electron-electron and electron-hole interactions, while better accounting for disorder and environmental screening in realistic interfaces, requires significant progress to improve both the accuracy and computational efficiency of available quantum simulation methods. In the present study, the results of different ab initio techniques are compared, namely time-dependent density functional and many-body perturbation theories, with experimental data on three different polymer/fullerene heterojunctions. It is shown that valuable information concerning the thermodynamic drive for electron-hole dissociation or recombination into triplets can be obtained from such calculations performed on model interfaces. In particular, the ability of these approaches to reproduce the Veldman and co–workers classification of the three studied interfaces is discussed, showing the success and limits of state-of-the-art ab initio techniques.

1. Introduction

Much attention has been devoted to gaining a better understanding of the structure–property relationships that govern the optoelectronic properties of novel organic materials for energy related applications. The photocurrent generation efficiency (i.e., the yield of free polarons) of organic photovoltaic devices depends critically on charge–separation processes at the interface between electron donor (D) and acceptor (A) phases. Moreover, in such systems, the nature and energy of fundamental physical processes (e.g., exciton diffusion and dissociation as well as charge carrier transport) are directly related to the chemical structure of the individual molecules/polymer chains and their microstructure organization. Charge transfer (CT) effects taking place at the donor–acceptor interface in organic photovoltaic materials are widely regarded as being crucial for the charge separation (CS) mechanism, and thus the power conversion efficiency of bulk–heterojunction (BHJ) organic solar cells. The small spatial confinement of the exciton, together with the low dielectric constant, ≈ 3 – 4, of organic semiconductors makes it seemingly difficult for the exciton to dissociate into separated charges, since the Coulomb electron–hole binding energy is supposedly high (0.4 – 1 eV), at least one order of magnitude larger than thermal energy at room temperature (~0.025 eV).[1–3] In photosynthesis, separation of charge carriers is achieved with the aid of cascaded energy levels and ion screening that additionally prevent charge recombination.[4,5] OPVs in contrast possess none of these elements, yet surprisingly, some OPV systems work very efficiently (with external quantum efficiency, EQE, up to 80% reported for the PCDTBT:PCBM blend).[6] The

Dr. D. Niedzialek
Now at Experimental Solid State Physics Group
The Blackett Laboratory
Imperial College
Prince Consort Road, London SW7 2BZ, UK
Dr. I. Duchemin
INAC, SP2M/L sim, CEA cedex 09, 38054 Grenoble, France
Dr. X. Blase
CNRS, Institut Néel, 38042 Grenoble, France
Univ. Grenoble Alpes
Institut Néel 38042, Grenoble, France
Dr. T. Branquinho de Queiroz, Prof. S. Kümmel
Theoretical Physics IV
University of Bayreuth
95440 Bayreuth, Germany
Dr. A. Rao, Prof. R. Friend
Optoelectronics Group Cavendish Laboratory
J J Thomson Avenue
Cambridge CB3 0HE, UK
Dr. S. Osella, Dr. D. Beljonne
Laboratory for Chemistry of Novel Materials
Center for Innovation and Research
in Materials and Polymers (CIRMAP)
University of Mons
20 Place du Parc 7000, Mons, Belgium
E-mail: David.Beljonne@umons.ac.be

DOI: 10.1002/adfm.201402682

fundamental question of how the organic heterojunction enables the electron and hole to overcome their mutual Coulombic attraction and achieve an efficient long–range charge separation, has remained a subject of intense scientific debate for more than a decade.[7–16]

One important question with regard to charge separation is the role of 'excess energy' ($\Delta G_{CT} = E_{CT1} - E_{S1}$) inherited from exciton generation upon light absorption. According to Veldman et al., ΔG_{CT} is the energy dissipated in the formation of the CT–state ($S_1 \rightarrow {}^1CT_1$); a negative value for ΔG_{CT} ensures the necessary driving force for the photoinduced electron transfer (PET) in a photovoltaic blend.[14] There are conflicting views on the role of ΔG_{CT}. In general, the energy of the absorbed photon above the optical gap is regarded as being wasted as heat. It has, however, been argued that this energy, which is lost during relaxation to the lower–lying ('cold') CT–state, facilitates long–range charge separation.[17,18] In contrast, Lee et al. in their work on polymer:fullerene heterojunctions (P3HT:PCBM and MDMO–PPV:PCBM) argued that 'hot'–exciton dissociation is not an important pathway for photocarrier generation and the role of excess energy remains unclear.[12] Lanzani and co–workers recently reported on ultrafast experimental investigations in PCPDTBT:PCBM blends showing that excess energy of the photon to promote high–lying, weakly–bound, excitons can actually be beneficial, as it increases the chances of the primary singlet excitons to split into free charges.[11] This is consistent with the earlier work of Köhler et al. on MEH–PPV, who resolved that a higher photocurrent can be generated by preparing the polymer chains in 'hot' exciton states with larger ionic character (and hence a higher propensity to split apart).[9] Grancini et al. attributed these faster kinetics to a higher degree of delocalisation of the 'hot' CT–states with respect to the 'cooled' ones, which is consistent with our previous quantum–chemical calculations and the work by Bakulin et al.[7,11] The spectroscopic results from Cambridge revealed that the long–range charge separation in efficient organic D:A photoconversion systems is mediated by the formation of higher–lying, delocalized electronic states rather than relaxation–assisted intermolecular hopping.[7] These 'hot' charge transfer states can be assessed experimentally by an infrared (IR) photon absorption, leading to 'hot'–state charge delocalization that may result in a decreased Coulomb binding and therefore possibly assist exciton dissociation into free carriers. The experimental results presented by Bakulin et al. indicate that the short time IR (~0.5 eV) optical excitation ('push'–pulse) of electron–hole pairs bound at the interface in a BHJ solar cell can take those excitations that had relaxed to 'cooled' bound CT–states back to states similar to the early–time 'hot' CT–states formed after the singlet excitation charge transfer, giving them a second chance to dissociate.[7] Our theoretical contribution to the work of Bakulin et al. using semi–empirical configuration interaction calculations supported their spectroscopic results, demonstrating that an optical excitation from a singly (positively) charged ground state to the lowest optically allowed electronic state (a transition from the polaronic to a delocalized band state in a one-electron picture) results in an increased intrachain hole delocalization for isolated polymer chains. Also, the charge density distribution of high–lying charge transfer excited states in polymer:C_{60} complexes was found to be more delocalized than the corresponding distribution in the lowest states. The experiments by Bakulin et al. on the same polymer–fullerene materials as Lee et al. indicated that 'pushed' ('hot') states are present also in these systems, though they might not play a major role in the charge separation process (which will ultimately be defined by the relative timescales for thermalization down to the 'cold' CT–state vs charge dissociation). Although the evidence coming from many new types of experimental and theoretical investigations points to the critical role of 'hot' charge transfer excitons in mediating the charge separation process, it likely coexists with other pathways (e.g., electric–field–assisted or energy barrier-less dissociation).[19–21]

The relative importance of charge separation pathways is expected to be material dependent and fixed by the interplay between several physical processes going on at organic heterojunctions, leading in turn to diverse quantum efficiencies for the corresponding organic photovoltaic cells (e.g., EQE measured by Bakulin et al. as 50%, 70% and 80%for PCPDTBT:PCBM, P3HT:PCBM and PCDTBT:PCBM blends, respectively, presented in **Figure 1**).[7] The full picture of the charge separation mechanism remains a mystery today, mainly

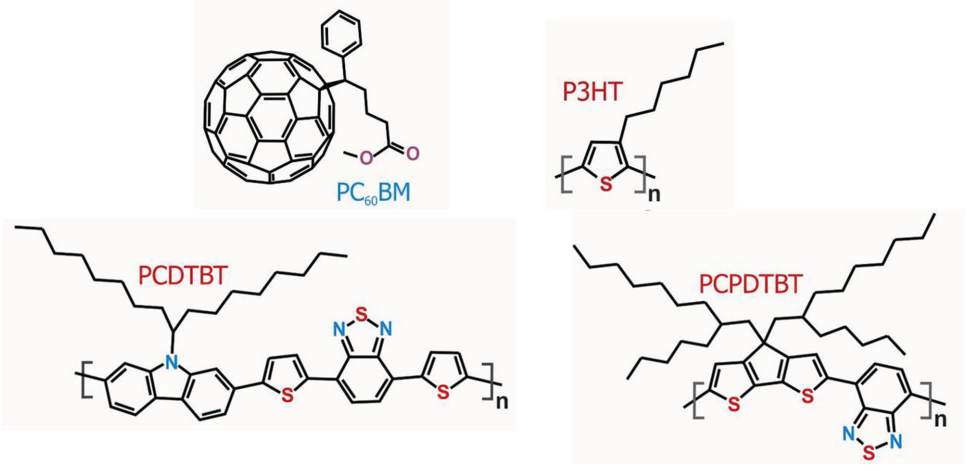

Figure 1. Chemical structures of donor (red captions) and acceptor (blue captions) organic materials investigated in this study.

due to a poor structural characterisation of the donor–acceptor interface.[7,11,12] Another important issue recently addressed by experimentalists, which directly relates to the energy of the charge–transfer states and the performance of organic photovoltaic devices, is the possibility that the CT excited state recombines into a neutral triplet excited state on one of the two materials ($CT_1 \rightarrow T_1$). The length scale of the separation between the two phases of the most efficient empirically optimized polymer:fullerene blends is similar to the exciton diffusion length (few nanometers), namely much smaller than the Coulomb capture radius (~16 nm) at room temperature for organic semiconductors. This causes a high rate of electron–hole encounters that could stay bound until recombination. The recombination of such Coulombically bound CT–states should in principle happen via formation of spin–triplet excitons, as in light–emitting diodes, and may represent a significant loss mechanism by reducing the photocurrent.[22,23] Fortunately, not every encounter leads to recombination and some OPV materials demonstrate mechanisms abating recombination and enhancing quantum efficiencies for charge separation. Charge recombination to triplets (CRT) has recently been identified for a number of D:A blends by Veldman et al.[14] The probability of various photoconversion channels, including recombination to the triplets, can be estimated from the state diagram with measured/calculated relative energetic positions of the lowest singlet (E_{S1}) and the lowest triplet (E_{T1}) on the donor/acceptor material and the charge–transfer (E_{CT1}) at the D:A interface. It has been shown by Veldman et al. that in order to prevent recombination to triplets, $-\Delta G_{CRT}$ must be lower than 0.1 eV, where $\Delta G_{CRT} = E_{T1} - E_{CT1}$ is the driving force for the CRT (**Figure 2**).[14]

In this work, we use a set of three first-principle approaches (TDDFT with B3LYP/6–31G(d,p), TDDFT with a non-empirically tuned range-separated hybrid functional (RSH), and many-body (GW–BSE) to unravel the nature and energy of electronic excitations (including higher excited states) in model complexes for the heterojunctions between (push–pull type) donor polymers and $PC_{60}BM$ acceptor. Initially, our main interest was in finding an appropriate quantum–chemical scheme that would be accurate enough while being practical to design criteria for state–of–the–art photovoltaic materials. We have thus started our investigation with the P3HT:PCBM interface model as a 'guinea pig' for testing the theoretical approaches. We have first performed a series of first–principles DFT/B3LYP calculations on this system and compare the results to those obtained from the much more expensive many-body GW/BSE approach and to experimental spectroscopic data on poly(3-hexylthiophene-2,5-diyl)P3HT:PCBM blends. Despite some differences, the two theoretical methodologies remarkably agree in predicting a manifold of CT–states with increasing electron–hole radii and in reproducing the magnitude of the driving force for charge separation. TDDFT based on the tuned RSH yields an overall picture for the electronic excitations that agrees with the GW/BSE predictions. We then applied these methods to address the importance of donor–acceptor energy mismatch in two high efficiency OPV heterojunctions: poly[N-9′-heptadecanyl-2,7-carbazole-alt-5,5-(4,7-di-2-thienyl-2′,1′,3′-benzothiadiazole] PCDTBT:PCBM and Poly[2,6-(4,4-bis-(2-ethylhexyl)-4H-cyclopenta[2,1-b;3,4-b′]dithiophene)-alt-4,7(2,1,3-benzothiadiazole)] PCPDTBT:PCBM, which have been designed to absorb in the long wavelength region of the solar spectrum and feature, therefore, a less favorable energy detuning (LUMO mismatch) for charge separation.

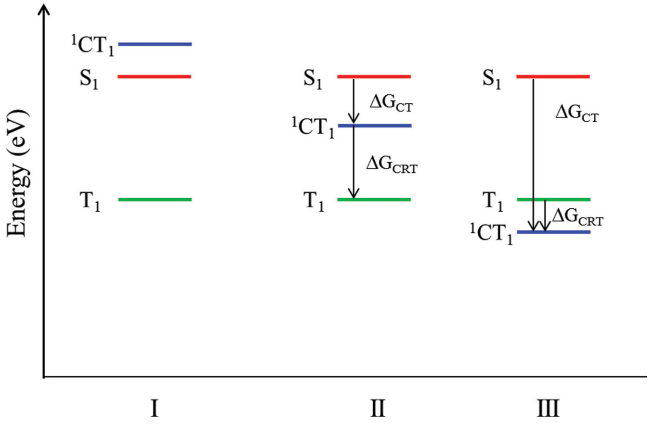

Figure 2. Energy diagram showing three possible arrangements of the lowest singlet (S_1), triplet (T_1), and $^1CT_1$ charge–transfer excited states relative to the singlet ground state for the three types of D–A blends according to Veldman et al.[14]: Type (I) represents D–A blends in which photoinduced electron transfer (PET) is absent because the $^1CT_1$ state is located at an energy higher than the lowest S_1 state. Types (II) and (III) show situations in which PET does occur: with (Type II) and without (Type III) charge recombination to the lowest T_1 state (CRT).

2. Results and Discussion

The chemical structures of the PCBM and polymers studied here are provided in Figure 1. Model complexes based on finite polymer chains interacting with a single fullerene derivative have been modeled, as detailed in the Methodology section.

2.1. P3HT: PCBM

From the optimized structure of the 10(P3HT):PCBM complex (10 denotes the number of monomers in the polymer chain), the lowest 20 electronic excitations have been computed at the TDDFT/B3LYP/6–31G(d,p) level. The lowest electronic excited state with a charge–transfer character ($^1CT_1$) calculated at about 1.1 eV, involves mainly a transition from the HOMO (lying on the polymer chain) to the LUMO (on PCBM), and together with the $^1CT_2$ (HOMO→LUMO+1) and $^1CT_3$ (HOMO→LUMO+2) contributes a set of three 'cold' charge-transfer excited states (**Figure 3**a and **Figure 4**). From the fourth excited state starts a bunch of 'hot' (CT) charge–transfer states, originating from deeper and more delocalized occupied molecular orbitals, mostly HOMO–1 ($^1CT_4$ – $^1CT_6$) and HOMO–2 ($^1CT_7$ – $^1CT_9$) (See the Supporting Information). They extend in energy up to ~2 eV, just below the on-chain HOMO→LUMO electronic transition to the S_1 state of P3HT, calculated at 2.05 eV, in excellent agreement with the experimental value of 1.91 eV.[24] In order to complete the energy state diagram, the transition energy to the polymer triplet (T_1) has been calculated at 1.31 eV, which is ~0.1 eV lower than the corresponding measured value (see Figure 3a and **Table 1**a).[22] Compared to experiment, the

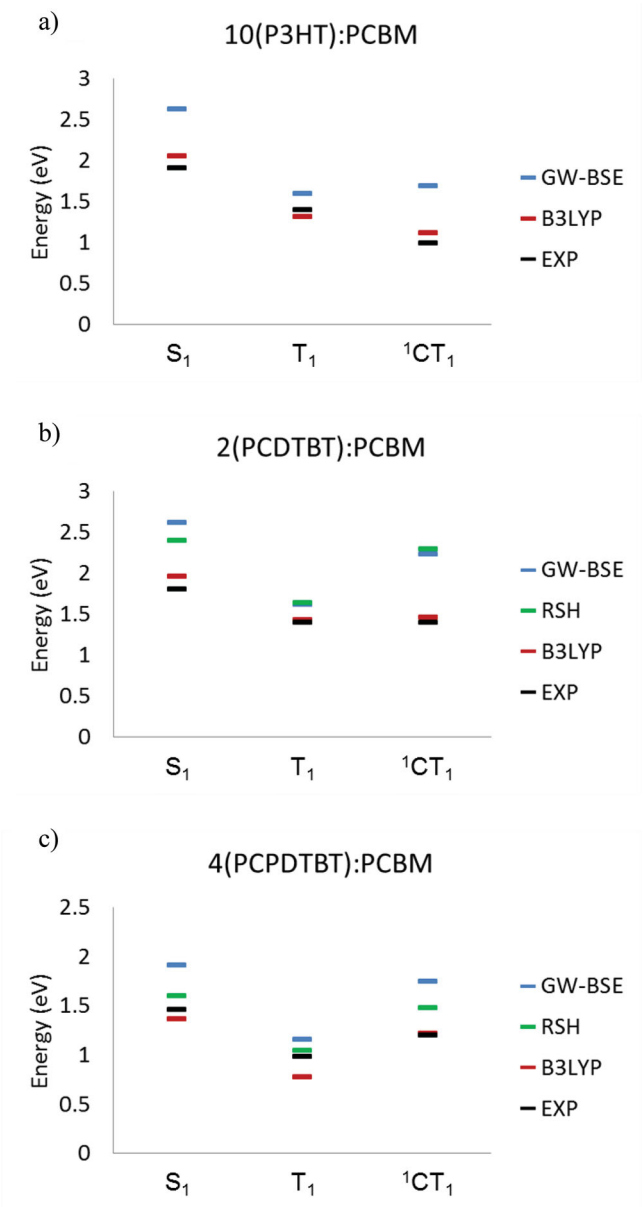

Figure 3. State diagrams of the energy alignment in the investigated systems: a) P3HT, b) PCDTBT and c) PCPDTBT blended with PCBM, as predicted by the GW/BSE, RSH and B3LYP methods, and as measured. S_1 and T_1 are the lowest–energy polymer singlet and triplet excitons, respectively. The $^1CT_1$ energy is the energy of the relaxed, Coulombically bound electron–hole pair across the heterojunction. The triplet $^3CT_1$ state is not presented here but its position has been calculated to be almost degenerated with the singlet $^1CT_1$ (see also Figure S10 for an extended energy diagram in the PCDTBT case).

DFT/B3LYP results for the P3HT:PCBM interface reproduce surprisingly well the relative position of the E_{S1}, E_{T1} and E_{CT1} on the energy state diagram (Figure 3a); in line with spectroscopic data, the P3HT:PCBM heterojunction is a clear example of a blend showing photoinduced electron transfer (PET) without subsequent charge recombination to the triplet (CRT) (Type III in Figure 2).[14] Complementing our theoretical results with more reliable self–consistent many–body GW/BSE calculations reveals a striking qualitative agreement between both levels of theory and the experimental observations. In spite of some (substantial) quantitative differences (see the SI), both theoretical methods match well in terms of the energy ordering of the most distinctive excited states (S_1/CT_1 alignment and the 'hot' CT–states lying below S_1 state), the topologies of the wavefunctions representing hole and electron, and the extent of delocalization in the 'hot' CT excited states (e.g., $^1CT_6$) with respect to the lowest–lying CT–state (e.g., $^1CT_1$). Although the excitation energies in the case of GW/BSE are hypsochromically shifted by ~0.5 eV with respect to the TDDFT/B3LYP values, there is excellent agreement in the driving force for PET (ΔG_{CT}), both fitting the experimental estimations of ca. –0.9 eV (Table 1a).[14] Also the TDDFT/B3LYP electron–hole separation as assessed from the state dipoles (**Figure 5**a) shows the same trend with excitation energy as the GW/BSE calculated electron–hole distances (Figure 5b). Both approaches suggest a rather modest increase of the electron–hole separation by ~1 – 2Å (according to GW/BSE) when going from the lower ($^1CT_1$ – $^1CT_3$) to the higher ($^1CT_4$ – $^1CT_6$) CT–states. This increase is more modest than that predicted from semi–empirical methods.[8] On this basis, we postulate that the relative delocalization in the 'cold' CT (e.g., $^1CT_1$) excited states in P3HT:PCBM heterojunction might promote substantial intermolecular electron–hole separations and increases the probability of free charge generation already from the lower–lying CT–states. We conclude from the study on P3HT:PCBM heterojunction that the lower–lying excited states ($^1CT_1$ – $^1CT_3$, blue colors in Figure S11a) are somehow delocalized and might promote long–range electron–hole separations, while there is only a limited increase in delocalization upon IR absorption from 'cold' to 'hot' CT–states. Note that: (i) this picture might be affected by the degree of intermolecular order in the P3HT– and/or PCBM–rich regions, which should generally lead to extended delocalization of the electronic states;[25] and (ii) localized excitations on the PCBM, labelled as S_i(PCBM) in what follows, are calculated to lie in between the singlet charge transfer $^1CT_1$ and polymer exciton S_1 state at both TDDFT and GW/BSE levels. The high PET driving force and the position of the 'hot' states just below the singlet S_1 state in P3HT:PCBM can promote effective pathway to the charge dissociation via 'hot' delocalized CT–states. Additionally, and in contrast to GW/BSE results (that yields a slightly positive value of ~0.09 eV), the lowest charge–transfer state is correctly predicted by B3LYP to be below the T_1 state ($-\Delta G_{CRT} = E_{CT1} - E_{T1} = -0.2$ eV), which is expected to cut off the $CT_1 \rightarrow T_1$ channel and suppress the losses via triplet recombination (Figure 3a). This, together with the high ΔG_{CT}, is usually invoked to explain the high external quantum efficiencies measured in P3HT:PCBM devices. The successful comparison of the TDDFT/B3LYP results and the experimental data for the P3HT:PCBM heterojunction, and the excellent agreement with GW/BSE calculations for the ΔG_{CT} charge-separation driving force, has encouraged us to investigate two other high efficiency low bandgap polymers presented in Figure 1, namely PCDTBT and PCPDTB.

2.2. PCDTBT: PCBM

Although blends of PCDTBT and PCBM are almost amorphous, these heterojunctions have been found to be more efficient

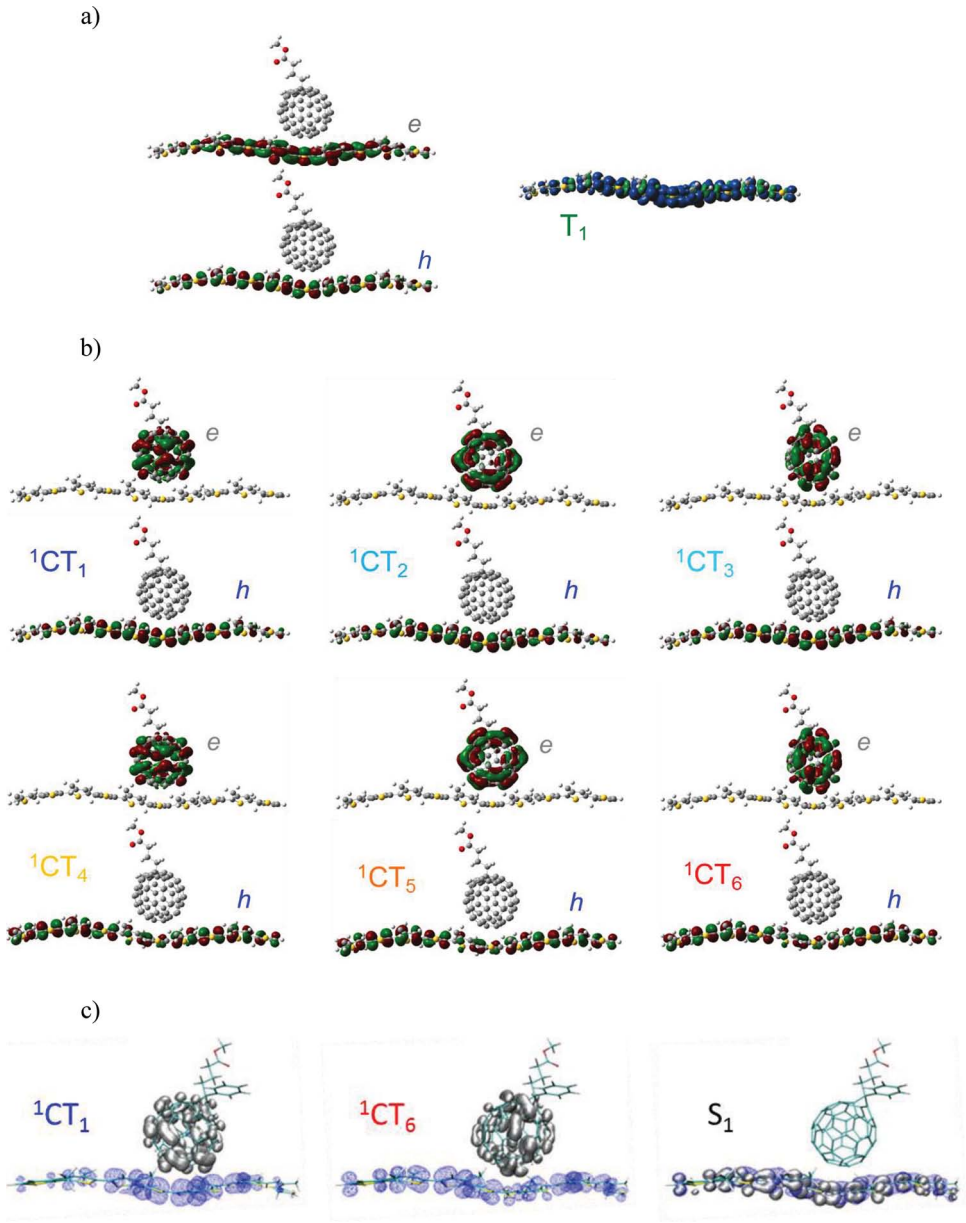

Figure 4. The topology of the excited states in a 10P3HT:PCBM complex. a) TDDFT/B3LYP calculated singlet (S_1) and triplet (T_1) states. For the triplet, we display the spin density calculated for the triplet ground state. b) For the TDDFT/B3LYP calculated singlets (S_1 and ^{1}CTs) we display the natural transition orbitals (NTO) for the hole (h) and electron (e). With light–dark blue colors we label the low–lying ('cold') ^{1}CT–states, while orange–red colors are used for the 'hot' ^{1}CT–states. c) 2-body electron-hole excited states calculated with the many-body BSE approach. Blue color is used for the (electron-averaged) hole and grey for the (hole-averaged) electron distribution. The left–to–right order is from lowest ($^1CT_1$) to highest in energy (S_1) states is in agreement with TDDFT/B3LYP results.

by 10% (EQE) in organic solar cells than the semicrystaline P3HT:PCBM heterojunction.[7] Two features are noticeable for PCDTBT: (i) the existence of a non–planar polymer backbone, which hinders the supramolecular organization of the stacking polymer chains; and (ii) too large spacing (~20 Å) between the alkyl side substituents that does not guarantee a patterned intercalation of the much smaller (~10 Å width) fullerene, desirable for structured interfaces. Despite these apparent unfavorable items on intermolecular organization, PCDTBT turns out to be a material of choice for OPV, which we thought might be inferred from a close inspection of the excited states formed at interface with fullerenes, see the energy diagram presented for 2(PCDTBT):PCBM in Figure 3b and Table 1b and wavefunction analysis in **Figure 6**. Here, we also include the results of tuned range–separated functionals, see also Figures S3-S10 and Table S10.

The comparison between the results obtained by the three different methods shows similitudes and differences: (i) the driving force for PET (ΔG_{CT}) predicted by B3LYP and GW/BSE calculations are in remarkable agreement, see Table 1b; (ii) the

Table 1. Experimental (EXP) and calculated (GW–BSE, RSH and B3LYP) energies of the relevant excited states (S_1, T_1,$^1CT_1$), exchange energy ($\Delta E_{ST} = E_{S1} - E_{T1}$) and driving forces ($\Delta G_{CT} = E_{CT1} - E_{S1}$ and $\Delta G_{CRT} = E_{T1} - E_{CT1}$), and assignment to a D–A blend type along the definition by Veldman et al. of the investigated blends (see Figures 2 and 3).

a) P3HT: PCBM							
Method	S_1 [eV]	T_1 [eV]	$^1CT_1$ [eV]	ΔE_{ST} [eV]	$-\Delta G_{CT}$ [eV]	$-\Delta G_{CRT}$ [eV]	TYPE
GW/BSE	2.62	1.60	1.69	1.02	0.93	0.09	II or III
TDDFT/B3LYP	2.05	1.31	1.12	0.74	0.93	–0.19	III
EXP[14]	1.91	1.4	0.99	0.51	0.92	–0.41	III
b) PCDTBT: PCBM							
GW/BSE	2.62	1.62	2.23	0.99	0.38	0.61	II
TDDFT/RSH	2.40	1.64	2.29	0.76	0.11	0.65	II
TDDFT/B3LYP	1.97	1.36	1.46	0.60	0.51	0.097	III
EXP	1.80	1.40	1.40	0.40	0.40	0	III
c) PCPDTBT: PCBM							
GW/BSE	1.91	1.16	1.74	0.75	0.17	0.58	II
TDDFT/RSH	1.60	1.04	1.48	0.56	0.12	0.44	II
TDDFT/B3LYP	1.36	0.77	1.22	0.59	0.14	0.45	II
EXP	1.46	0.98	1.20	0.48	0.26	0.22	II

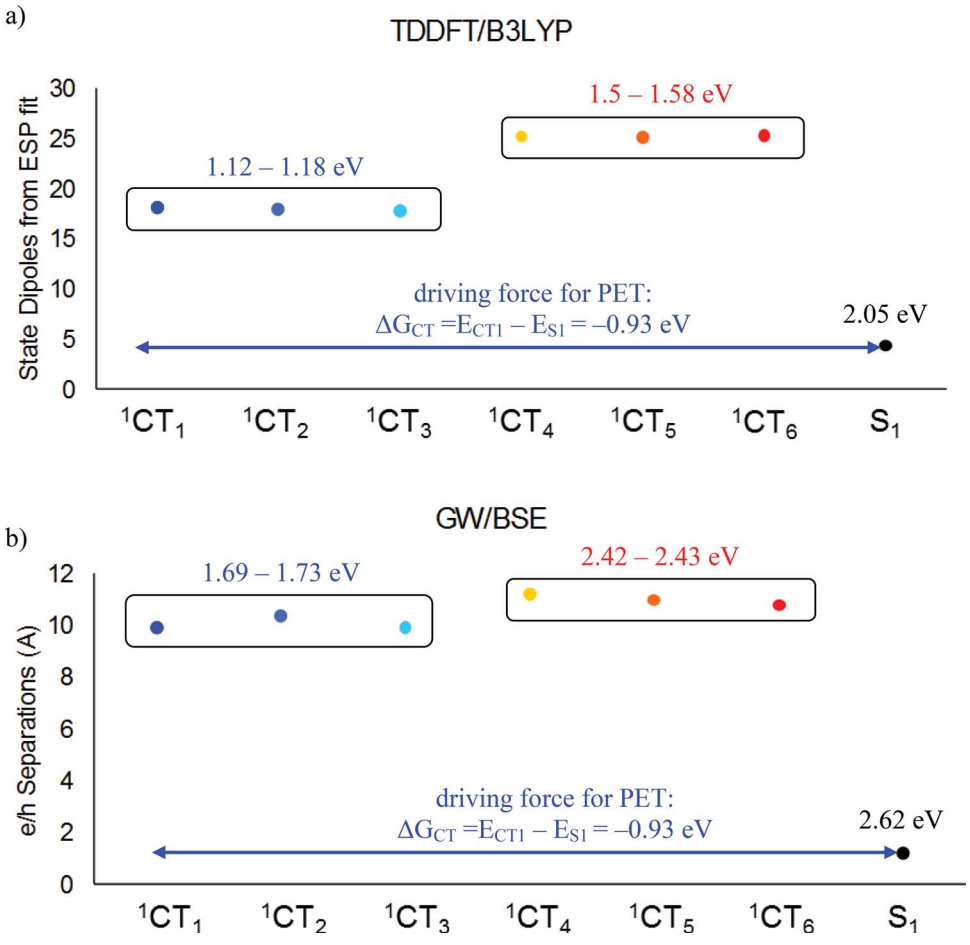

Figure 5. a) TDDFT/B3LYP state dipoles and b) GW/BSE electron–hole separation for relevant excited states in the 10P3HT:PCBM complex. The blue arrows represent the driving force calculated with both methods. Both approaches suggest a modest (~2 Å, according to GW/BSE) increase in the electron–hole separation when going from the lower to the higher–lying CT–states.

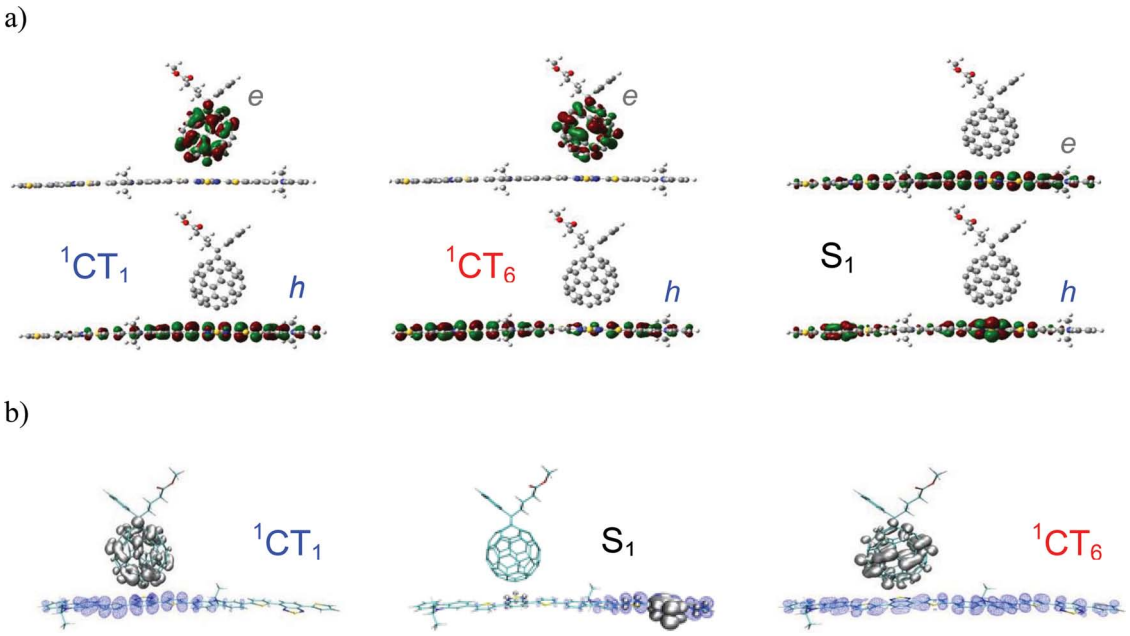

Figure 6. The topology of the relevant excited states in a 2(PCDTBT):PCBM complex, as calculated with a) TDDFT/B3LYP and b) many body ab–initio GW/BSE approaches. The holes and electrons are represented as in Figure 4. The left–to–right order is from lowest ($^1CT_1$) to highest in energy.Note that according to the TDDFT/B3LYP results, the S_1 state lies above the 'hot' ^1CT states (e.g., $^1CT_6$), while it is below from GW/BSE calculations.

lowest electronic excitations confined over the fullerene derivative, S_i(PCBM), are located *above* the first CT state in TDDFT/B3LYP, yet *below* it from both GW/BSE and tuned RSH calculations (Table 1b); (iii) while GW/BSE and RSH TDDFT place the lowest polymer confined triplet excited state, T_1, well above the lowest singlet charge-transfer state, these two states are almost degenerate at the B3LYP level. We will come back later to these differences, which clearly arise from the different propensities of the methods to (over)stabilize either intra- or inter-molecular charge transfer excitations and concentrate here below on the B3LYP results that, surprisingly, provide the most consistent picture when compared to experiments.

From B3LYP calculations thus, PCDTBT:PCBM blends also belong to Type III heterojunctions but with the driving force for PET about twice smaller in comparison to P3HT:PCBM. The GW/BSE results again show the same behavior with a ~2.4 eV reduction of the ΔG_{CT} driving force as compared to P3HT (see Table 1b). The B3LYP value of ΔG_{CRT} = 0.097 eV is in excellent agreement with the measured close to zero T_1–CT_1 energy window, which should efficiently diminish recombination to triplets.[14,22] Yet, this mechanism might be less effective than in the P3HT:PCBM blend, in which the T_1 energy level is well above the lowest charge–transfer state (Figure 3b and Table 1b).

The sequence of the photophysical processes in the Type III heterojunction can be rationalised as a (i) photoexcited creation of a singlet exciton (S_1) followed by (ii) its ionization at the heterojunction, leading to (iii) the formation of delocalized 'hot' CT–states.[7,11] In PCDTBT:PCBM heterojunction (similarly to P3HT:PCBM blend), these intermediate 'hot' delocalized charge–transfer states lie below the S_1state (from B3LYP), which should favor processes (ii) and (iii) and efficient separation into free charges. Now, if bimolecular recombination of electrons and holes occurs, it would lead to the formation of charge–transfer states with both spin–singlet ($^1CT_1$) and spin–triplet ($^3CT_1$) characters (in a 1:3 ratio, as mandated by spin statistics), which are almost degenerate in energy.[26,27] The $^1CT_1$ state can recombine to the ground state. The recombination from the $^3CT_1$ state to the ground state is spin–forbidden, but if transition to the T_1 state is energetically accessible ($-\Delta G_{CRT} > 0.1$ eV), triplet excitons can return to the ground state via a radiative decay channel or by triplet–charge annihilation.

Additionally, relatively closer energies of $^1CT_1$ and $^3CT_1$ with respect to S_1 can increase the probability of recycling (under advantageous conditions, *e.g.* thermal energy)[17] these charge–transfer states back to free charges. Although the PCDTBT:PCBM heterojunction belongs to Type III blends with ability to restrain the CRT process, clearly this feature cannot be the only reason of its excellent efficiency, even higher than that for the well–crystallizing type III polymer, P3HT, which besides sustains a twice larger PET driving force at fullerene interface. That moved our attention again towards the delocalization issue. Already the plot of the relative charge distribution per polymer unit shows a drastic difference with respect to the P3HT:PCBM complex (Figure S11b).

Large (with respect to the P3HT case) changes in the charge distribution along the copolymer chain in all the analysed excited states are associated with the presence of alternating electron–rich (donor) and electron–poor (acceptor) moieties. We observe a pronounced shift of the positive charge from the region below the PCBM (Figure S11b) towards the end of the polymer chain, suggesting a hole delocalization and, in turn, increased separation from the electron in the 'hot' charge–transfer states. In line with this finding, there is a drastic increase in the GW/BSE hole–electron separation radius (by ~7Å) and TDDFT state dipole moment when going from lower- to higher-lying charge–transfer states (e.g., from $^1CT_1$ to

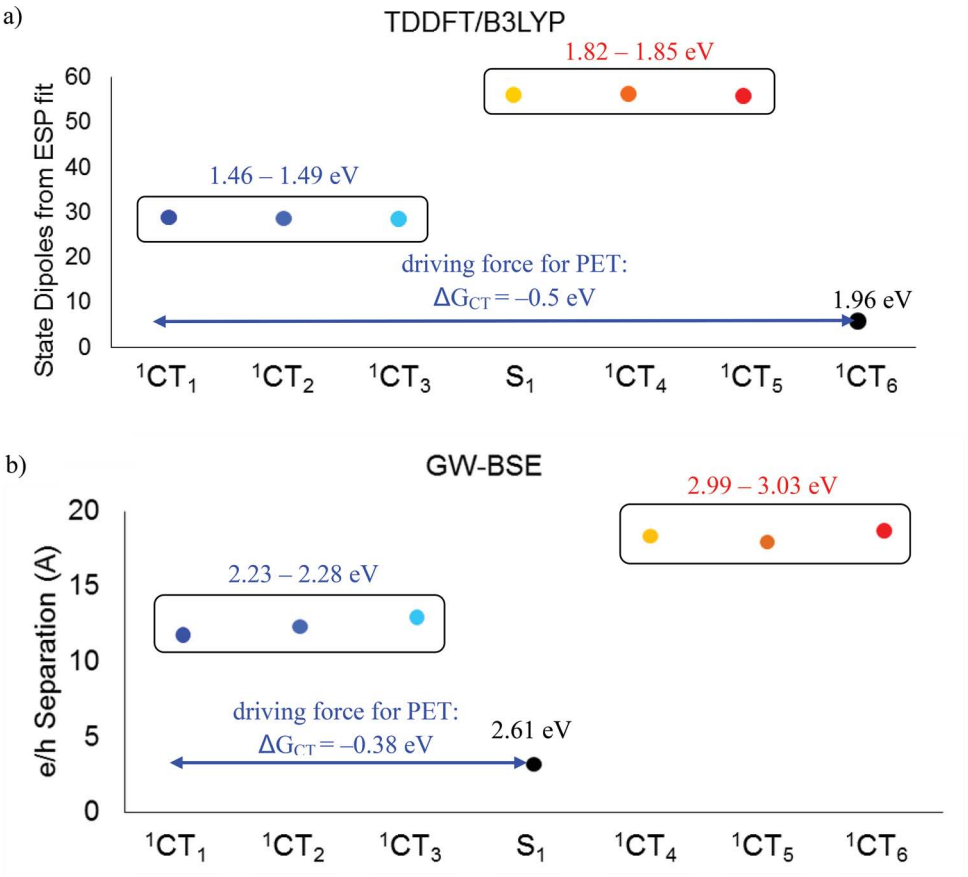

Figure 7. a) TDDFT/B3LYP state dipoles and b) GW/BSE electron–hole separation for relevant excited states in the 2(PCDTBT):PCBM complex. The blue arrows represent the driving force calculated with both methods. Both approaches suggest a drastic (~7 Å, according to GW/BSE) increase in the electron–hole separation when going from the lower to the higher–lying ^{1}CT–states. Note the difference in the relative energy ordering between the high-lying ^{1}CT excited states obtained from TDDFT/B3LYP and GW/BSE.

$^1CT_6$, see **Figure 7**). It can thus be inferred that the outstanding quantum efficiency (EQE) of the PCDTBT:PCBM heterojunction at least partly arises from the advantageous interplay between the following three factors: (i) The energetics of this interface, with a number of 'hot' CT–states lying below the S_1state together with a relatively high PET driving force, promotes multiple efficient pathways for dissociation through delocalized CT states. (ii) The much enlarged electron-hole radii in the 'hot' CT–states that is associated with shifting the hole between successive carbazole electron-poor units along the D-A conjugated backbones. (iii) The relative position of the T_1 state versus the charge–transfer states, which restrains the recombination to triplets and may increase the probability of recycling the Coulombicaly bound charge–transfer states back to free charges.

2.3. PCPDTBT: PCBM

The PCPDTBT copolymer (Figure 1) is widely known for its extraordinary hole transport abilities, showing high–crystallinity in blends with PCBM.[28,29] Therefore, a relatively low EQE efficiency of only 50% of the PCPDTBT:PCBM heterojunction–based OPV devices can be considered as a surprisingly disappointing result, as undoubtedly structural organization should favor dissociation at PCPDTBT:fullerene heterojunctions. Indeed, the planar backbone of the polymer promotes the supramolecular organization of the stacking polymer chains into ordered structures and the spacing between the side alkyl substituents of ~14 Å does guarantee a patterned intercalation of the $PC_{60}BM$ or $PC_{70}BM$ (~10 and ~13 Å width, respectively) fullerene derivatives. Also PCBM efficiently forms large aggregates, which should additionally improve the charge separation due to delocalization of the electron wavefunction over the fullerene aggregates.[25,30] Although PCPDTBT and PCBM intermix together very well into a semi–crystalline blend, their EQE is much lower than that reported for the amorphous PCDTBT–blend. The energetic profile for the lowest electronic excitations inthe 4(PCPDTBT):PCBM complex (Figure 3c and Table 1c) much differs from the two previously analyzed 'Type III blends', as it belongs to another type (Type II) in the Veldman et al. classification (from B3LYP: $-\Delta G_{CRT} = E_{CT1} - E_{T1} \approx 0.2$ eV > 0.1).[14]

Moreover, as shown in Figure 3c, a photoexcited singlet exciton on the polymer (S_1) is unlikely to open up pathways involving 'hot' delocalized CT states (mediating the charge separation), in contrast to what has been found for P3HT- and PCDTBT–fullerene blends. This is due to the relative ordering

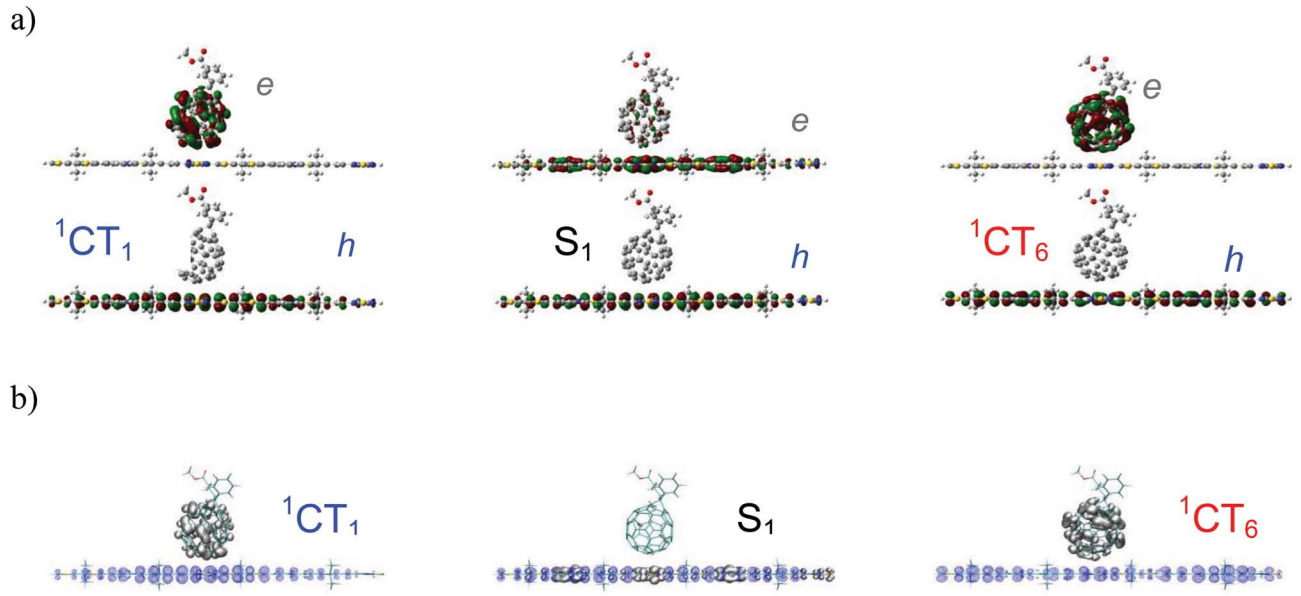

Figure 8. The topology of the relevant excited states in a 4PCPDTBT:PCBM complex, as calculated with a) TDDFT/B3LYP and b) many body ab–initio GW/BSE approaches. The holes and electrons are represented as in Figure 4. The left–to–right order is from lowest ($^1CT_1$) to highest in energy ($^1CT_6$) states. The relative energy orderingsof the states predicted from GW/BSE and TDDFT/B3LYP are consistent.

of the charge–transfer excited states with the 'hot' CTs lying now *above* the polymer S_1 singlet, see **Figure 8**. Furthermore, our calculations indicate that T_1 has a lower energy than the singlet ($^1CT_1$) and triplet ($^3CT_1$) charge–transfer states. Once formed, triplet excitons can return to the ground state through radiative decay or via a triplet–charge annihilation channel. In addition to the open channel for the recombination to triplets (Type II system), also the PET driving force is very unfavorable, almost seven times smaller than for P3HT. The only modest EQE for PCPDTBT:PCBM blend thus possibly stems from both its disadvantageous energy profile (small ΔG_{CT} and the 'hot' CTs lying higher in energy than S_1) and a strong loss mechanism via severe recombination to triplets ($-\Delta G_{CT} > 0.1$ eV).

As in the P3HT:PCBM complexes, our results point to a substantial hole delocalization in the lower–lying charge–transfer states (e.g., $^1CT_1$, Figure S11c) of PCPDTBT:PCBM, which is consistent with the excellent hole transport properties of that semi-crystalline polymer. The spatial extent of the hole–representing wavefunction is slightly increased from the 'cold' CT to the 'hot' CT and similarly accounted for at different levels of theory (TDDFT/B3LYP and GW/BSE). Further analysis of the relative charge distribution per polymer unit (Figure S11c) and inspection of the electron–hole separation diagrammatic pictures (Figure 8) confirm our expectations based on the shape of the hole NTO–wavefunctions (**Figure 9**). The fluctuations inthe excess charge distribution along the polymer chain can be traced back to the presence of alternating electron–rich (donor) and electron–poor (acceptor) moieties (as in PCDTBT). Yet, as in P3HT, the charge is relatively delocalized already in the lowest CT states. This is the reason why the increase of the electron–hole separation is so small (~1 Å, according to GW/BSE calculations) when going from 'cold' to 'hot' CT–states.

The final picture of the PCPDTBT:PCBM heterojunction emerging from our calculations shows that there are few disadvantageous aspects related to the excited-state energetics that potentially hinder high efficiencies, namely: (i) the relative position of the T_1 state – lower in energy than the singlet ($^1CT_1$) and triplet ($^3CT_1$) charge–transfer states, thereby opening new channels for the recombination to the T_1 triplet. This has been recently explained by Rao et al. as the main loss mechanism in the PCPDTBT:PCBM blend.[22] (ii) The other serious drawback of this interface is the energy unfavorable dissociation pathway via 'hot' delocalized states. These are partly compensated by the good crystallization properties of the PCPDTBT polymer and its ability of intercalation or enabling the formation of fullerene aggregates between the polymer side chains.

3. Conclusions

We have used time-dependent density functional theory (TDDFT) with the B3LYP and a tuned RSH functional, and the GW-BSE approach, to assess the nature and energetics of relevant excited states at three representative polymer/fullerene interfaces, involving P3HT, PCDTBT or PCPDTBT as donor and $PC_{60}BM$ as acceptor. In organic solar cells the photocurrent generation efficiency depends critically on charge separation processes which, in turn, are sensitive to both (i) the chemical structure of the donors and acceptors and (ii) the microstructural organization of the heterojunctions. Our TDDFT/B3LYP studies reveal that charge separation efficiency and, in turn device performance, are influenced by electronic energy level alignment at interfaces, degree of delocalisation of the excited states – and hence crystallinity – and competition with loss processes such as recombination to triplets. The three polymers here studied show interesting differences in external quantum efficiencies (EQE) when blended with the same fullerene acceptor. We present in **Figure 10** an attempt to correlate the

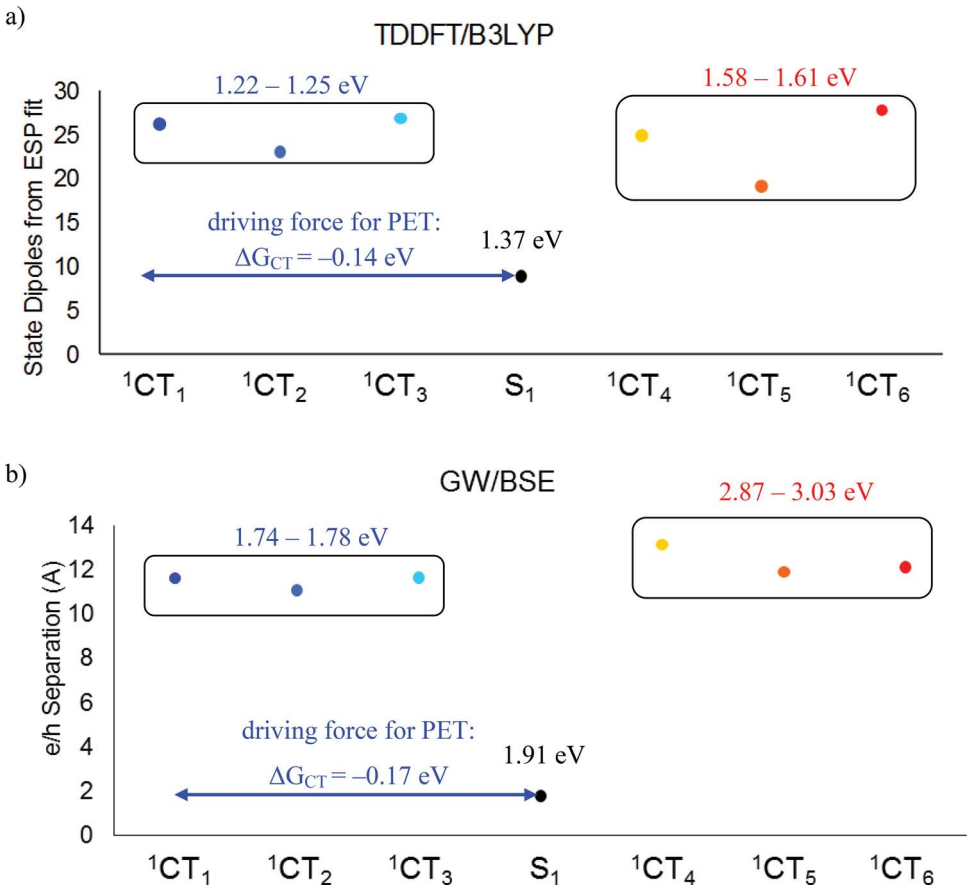

Figure 9. a) TDDFT/B3LYP state dipoles and b) GW/BSE electron–hole radii in the 4PCPDTBT:PCBM complex. The blue arrows represent the driving force energy for PET. Both approaches suggest a negligible increase of the electron–hole separation going from the lower to the higher–lying ^{1}CT–states,by only (according to GW/BSE) ~1Å.

measured OPV performances to B3LYP calculated excited-state features including energy level alignment and delocalisation of the hole in 'cold' and 'hot' charge-transfer states.

Despite favorable microstructure properties (high polymer crystallinity and intercalation of PCBM between the polymer side chains), PCPDTBT:PCBM blends feature a modest EQE of ~50%. We speculate below on the origin of such a low EQE. First, we notice that the driving force for charge separation via the 'cold' CT states is small, while the higher–lying CT states are energetically not accessible from the lowest polymer singlet S_1 state. In addition, the molecular triplet (T_1) on the donor lies energetically below the $^1CT_1$. These features, which are typical for large open-circuit voltage heterojunctions, are detrimental to photocurrent as they limit charge separation and favor recombination into triplets. At the other extreme, the P3HT:PCBM bulk heterojunction is a representative case of a low V_{OC} interface withan intermediate EQE of ~70%. There, TDDFT B3LYP results provide electronic states spanning the large (~0.9 eV) energy window between the polymer singlet and the lowest CT state where hole delocalization along the polymer backbone could mediate exciton dissociation (in both 'cold' and 'hot' CT states, with only a modest increase of the electron-hole radius with increasing energy); at the same time, recombination into molecular triplets is a high-T thermally activated process. In comparison to the two cases above, the PCDTBT:PCBM complex appears as an ideal intermediate case in terms of the energy level alignment for the following reasons: (i) this is a high V_{OC} heterostructure, yet one where the molecular triplet state is not significantly downshifted below the lowest CT state; and (ii) though the driving force for charge separation is reduced compared to P3HT:PCBM, higher-lying 'hot' CT states are energetically accessible and can potentially intercede in the dissociation mechanism. Most importantly, the hole wavefunction in these CT states has large contributions over the carbazole units, so that the average electron-hole radii substantially increase when going from 'cold' to 'hot' CT states, as this primarily involves a shift of the hole density along the polymer backbone.

We conclude with a short discussion on the comparison between the results provided by the different theoretical approaches adopted here. It is well documented that, mostly owing to the self-interaction error and the too short-sighted exchange-correlation potential, TDDFT/B3LYP underestimates the energy of charge transfer excitations.[31–33] However, medium dielectric polarization effects, not included here, also largely renormalize the electronic bandgap upon going from isolated molecules to the corresponding solid-state materials; typical electronic polarization energies in organic conjugated

Material's Characteristics:		P3HT	PCDTBT	PCPDTBT
Hole mobility of the polymer[14,47] (cm^2/Vs)		10^{-1}	10^{-5}	10^{-4}
EQE in blend with PCBM[7] (%)		70	80	50
The open circuit voltage, V_{OC}[14,47] (V)		0.61	0.89	0.62
STRUCTURE	High Crystallinity of the Polymer	**YES**	NO	**YES**
	Intercalation of PCBM between the Polymer Side Chains	NO	NO	**YES**
ENERGETICS	High PET Driving Force $E(S_1 - {}^1CT_1)$	**YES**	**YES**	NO
	Accessed 'hot' States (below S_1)	**YES**	**YES**	NO
	Suppressed Recombination to the Triplets: $E({}^1CT_1 - T_1) < 0.1$ eV	**YES**	**YES**	NO
CHARGE LOCALISATION	Delocalized Positive Charge on the Polymer in the 'hot' States	**YES**	**YES**	**YES**
	Increased e/h Separation in the 'hot' States	NO	**YES**	NO

Figure 10. Schematic representation of the main features of the investigated interfaces from TDDFT/B3LYP calculations.

crystals are in the ~1 eV range, so that a free charge-transfer pair is expected to be stabilized by up to 2 electron-volts when embedded in the polarizable environment of the surrounding conjugated chromophores.[20,21] From the study of the model systems investigated here, it seems these two main sources of errors (local character of the kernel and lack of polarization effects) almost perfectly cancel out, providing an overall energetic scheme for the local vs charge-transfer excitations in gas-phase model complexes in excellent agreement with the measured spectroscopic data on the corresponding bulk heterojunctions. While this is good news as it validates the relatively inexpensive gas-phase B3LYP approach to perform fast screening calculations of potentially interesting donor–acceptor interfaces, one must keep in mind that the quantitative agreement with experiment obtained here for B3LYP results is borne out by a lucky cancelation of errors.

At a higher level of theory, GW/BSE and range-tuned TDDFT provide in all cases investigated here fully consistent pictures both qualitatively (ordering of the relevant electronic excitations) and quantitatively (very similar excitation energies). Compared to B3LYP and experiment, the best agreement to the gas-phase GW/BSE and RSH TDDFT values is obtained, not surprisingly, for vertical transition energies to local, highly covalent, electronic excited states, namely the spatially confined polymer triplet and PCBM singlet molecular excitons. Interestingly, the GW/BSE transition energies to 'moderately' ionic excited states such as the on-chain S_1 and the lowest ('cold') inter-chain charge-transfer excitons seem to be similarly affected by the neglect of environmental polarization effects, as their energy difference—namely the dissociation driving energy—was found to be very close to both the B3LYP and the experimental results in the three complexes investigated. Charge-transfer states with larger ionic character, such as the 'hot' CT states in PCDTBT:PCBM, are, however, predicted too high in energy from GW/BSE calculations, clearly an outcome of the incomplete dielectric screening accounted for in our polymer-fullerene complex calculations.

This calls for the development of embedding techniques, such as the family of continuous polarizable models (PCM) or discrete microelectrostatic models, to be adapted to the Bethe-Salpeter formalism, which should allow to treat on an equal footing all electronic excitations in complex multi-chromophoric systems, from the most covalent to the most ionic. In this regard, we would like to point to the very recent and elegant work by Baumeier et al. who combined many-body Green's function theory to a polarizable environment in a lattice model.[34] The combination of TDDFT using tuned RSH functional and PCM models has recently been explored by some of us.[35]

4. Experimental Section

The GW and Bethe-Salpeter (BSE) methods, which belong to the family of many-body Green's function perturbative techniques,[36] are expected to give accurate estimations of the Frenkel and CT–state energies, as these take into account many–body effects and electron–hole interactions. They have been shown recently to provide inter- or intra-molecular charge-transfer excitation energies in good agreement with experiments or higher-level (CASPT2) calculations in a few prototype gas phase organic systems such as model donor–acceptor dimers, polypeptides or coumarin dyes.[37–40] In such systems, the agreement with optimized range-separated hybrids TDDFT calculations was also shown to be excellent, with discrepancies no larger than 0.1–0.2 eV. Technical details about the present implementation within the Fiesta code can be found in Refs. [37–38] and in the SI. However, since calculations are performed in the gas phase (isolated complexes) and provide vertical values, one may certainly expect computed excitations energies in excess of their experimental counterparts.

A perceived drawback of the GW methodology is its computational cost, usually thought to be an order of magnitude more expensive than a typical TDDFT calculation. The large computational effort associated with the GW/BSE method has limited these calculations to rather moderately simple systems up to few hundred of atoms. For this reason, our models of BHJ interfaces have been limited to oligomer:fullerene complexes. Opportunely, they were able to represent sufficiently all studied interfaces in terms of the characteristics of the most relevant excited states and to extract useful energetic trends that were confronted to B3LYP TDDFT and experimental results. For consistency between the models (due to different monomer length of each investigated polymer), we used a dimer chain to model PCDTBT and a tetramer for PCPDTBT, as these are the oligomer lengths for which we observe a saturation in the values of the crucial size–dependent electronic properties for these systems. In order to obtain a reliable model of the π–stacking dimer geometry, all structural optimizations have been performed using an empirical long–range correlation corrected functional with dispersion correction (ωB97XD/6–31G(d,p)). Such a functional is expected to give more physically meaningful predictions for systems composed of weakly interacting molecules compared to other DFT approaches or force–field methods, which tend to overestimate the π–stacking distance. After optimizing the geometries of the isolated polymer chains and the polymer:PCBM complexes, the backbones of PCDTBT and PCPDTBT models were planarized. The π–stacking distance was fixed at ~3.5 Å in all cases (accordingly to the ωB97XD optimized values) and the final position of the PCBM has been chosen in the spacing between the side alkyl chains.

The preliminary qualitative evaluation of the nature of the adiabatic electronic states is visual, and based on shape of hole/electron densities represented by the natural transition orbitals (NTOs) isosurfaces. In order to address the interchain delocalization of the charge transfer state, the electron–hole separation is estimated from the state dipole value of a given excited state at the B3LYP level, and directly compared with the GW/BSE calculated electron–hole separation for the corresponding excited-state 2-body wavefunctions. Furthermore, for each electronic excited state obtained from TDDFT simulations of the polymer:PCBM complexes, we estimate the degree of the positive charge delocalization on the conjugated chain by summing the electrostatic potential (ESP) fitted partial charges for the excited states (ES) over donor molecule and subtracting the corresponding ground state (GS) ESP charge. The (ES – GS) ESP charge distribution gives us a measure of the degree of both intra– and interchain delocalization in the 'cold' vs 'hot' charge transfer states. It helps to understand the nature of these excited states and to project how they could act in overriding the Coulomb interaction in the modelled polymer:fullerene blends.

DFT and TDDFT RSH calculations were performed using the range separated hybrid functional ωPBE[41] with the range-separation parameter non-empirically adjusted such that the HOMO eigenvalue and the IP resulting from a ΔSCF calculation agree as closely as possible.[42] The details of the tuning procedure are given in the Supporting Information. It has been repeatedly demonstrated that TDDFT with tuned RSH functional predicts CT excitations reliably[42–44] and yields generalized Kohn-Sham eigenvalues that often correspond closely to the quasi-particle excitations of GW calculations.[42] This goes beyond what can be achieved with "traditional" density functional, such as generalized gradient approximations, and there are at least two reasons for this success. First, through the use of the Generalized Kohn-Sham scheme (part of) the exchange-correlation derivative discontinuity effects are built into the DFT eigenvalue spectrum.[42] Second, by adjusting the range separation parameter such that the HOMO eigenvalue becomes identical to the first ionization potential, the functional incorporates screening effects in a controlled and system specific way, thus capturing an important aspect of electron correlation. Since screening effects are also decisive in the GW approach, the close correspondence between GW and tuned RSH results is not a coincidence. In our present study TDDFT with the tuned RSH impressively confirms the picture that GW/BSE yields for the electronic excitations. Finally, we perform more standard TD-B3LYP calculations with the 6–31G(d,p) basis. As discussed here above, even though less accurate for calculating vertical transition energies than GW/BSE or TD-RSH techniques, TD-B3LYP calculations benefit, when performing comparisons between gas phase calculations and bulk measurements, from significant error cancellations between missing bulk screening effect and the underestimation of CT excitation energies due to the lack of proper long-range exchange.

Experimentally, S_1 energies of PCDTBT and PCPTDBT were obtained from the absorption onset and found to match previously reported values.[14] The CT energies were obtained from the peak of the CT state emission, measured by photoexciting thin films of the polymer-fullerene blend above the bandgap and monitoring the weak luminance from CT state recombination. The values obtained agree with previous reports.[45,46] The T_1 energy of PCPDTBT has been reported by Janssen and co-workers.[45] P3HT:PCBM blend in a 1:1 ratio and PCDTBT:PCBM blends in a 1:4 ratio were considered.

Acknowledgements

X.B. acknowledges the French National Research Agency (ANR-2012-BS04 PANELS) and computing time from the French GENCI (No i2012096655) and European PRACE (No. 2012071258) programs. S.K. and T.B.d.Q. acknowledge financial support from the Bavarian State Ministry of Science, Research, and the Arts for the research network "Solar Technologies go "Hybrid". The work in Mons has been supported by the Interuniversity Attraction Pole programs of the Belgian Federal Science Policy Office (PAI 7/05) and by FNRS-FRFC. D.B. is a FNRS Research Director. The project UPGRADE acknowledges the financial support of the Future and Emerging Technologies (FET) programme within the Seventh Framework Programme for Research of the European Commission, under FET-Open grant number: 123456.

Received: August 7, 2014
Revised: September 8, 2014
Published online: October 2, 2014

[1] A. Koehler, H. Baessler, *Mater. Sci. Eng. R* **2009**, *66*, 71.
[2] G. D. Scholes, G. Rumbles, *Nat. Mater.* **2006**, *5*, 683.
[3] A. C. Morteani, P. Sreearunothai, L. M. Herz, R. H. Friend, C. Silva, *Phys. Rev. Lett.* **2004**, *92*, 247402.
[4] R. E. Blankenship, *Molecular Mechanisms of Photosynthesis*, (Blackwell Science, Oxford, **2002**).
[5] M. R. Jones, *Biochem. Soc. Trans.* **2009**, *37*, 400.
[6] S. H. Park, A. Roy, S. Beaupré, S. Cho, N. Coates, J. S. Moon, D. Moses, M. Leclerc, K. Lee, A. J. Heeger, *Nat. Photonics* **2009**, *3*, 297.
[7] A. A. Bakulin, A. Rao, V. G. Pavelyev, P. H. M. van Loosdrecht, M. S. Pshenichnikov, D. Niedzialek, J. Cornil, D. Beljonne, R. H. Friend, *Science* **2012**, *335*, 1340.

[8] T. Strobel, C. Deibel, V. Dyakonov, *Phys. Rev. Lett.* **2010**, *105*, 266602.
[9] A. Köhler, D. A. dos Santos, D. Beljonne, Z. Shuai, J.-L. Brédas, A. B. Holmes, A. Kraus, K. Müllen, R. H. Friend, *Nature* **1998**, *392*, 903.
[10] A. E. Jailaubekov, A. P. Willard, J. R. Tritsch, W.-L. Chan, N. Sai, R. Gearba, L. G. Kaake, K. J. Williams, K. Leung, P. J. Rossky, X.-Y. Zhu, *Nat. Mater.* **2013**, *12*, 66.
[11] G. Grancini, M. Maiuri, D. Fazzi, A. Petrozza, H.-J. Egelhaaf, D. Brida, G. Cerullo, G. Lanzani, *Nat. Mater.* **2013**, *12*, 29.
[12] J. Lee, K. Vandewal, S. R. Yost, M. E. Bahlke, L. Goris, M. A. Baldo, J. V. Manca, T. van Voorhis, *J. Am. Chem. Soc.* **2010**, *132*, 11878.
[13] V. I. Arkhipov, P. Heremans, H. Baessler, *Appl. Phys. Lett.* **2003**, *82*, 4605.
[14] D. Veldman, S. C. J. Meskers, R. A. J. Janssen, *Adv. Funct. Mater.* **2009**, *19*, 1939.
[15] A. A. Bakulin, D. Martyanov, D. Y. Paraschuk, P. H. M. van Loosdrecht, M. S. Pshenichnikov, *Chem. Phys. Lett.* **2009**, *482*, 99.
[16] R. A. Marsh, J. M. Hodgkiss, R. H. Friend, *Adv. Mater.* **2010**, *22*, 3672.
[17] S. Shoaee, T. M. Clarke, C. Huang, S. Barlow, S. R. Marder, M. Heeney, I. McCulloch, J. R. Durrant, *J. Am. Chem. Soc.* **2010**, *132*, 12919.
[18] R. D. Pensack, J. B. Asbury, *J. Am. Chem. Soc.* **2009**, *131*, 15986.
[19] D. Veldman, O. Ipek, S. C. J. Meskers, J. Sweelssen, M. M. Koetse, S. C. Veenstra, J. M. Kroon, S. S. van Bavel, J. Loos, R. A. J. Janssen, *J. Am. Chem. Soc.* **2008**, *130*, 7721.
[20] F. Castet, G. D'Avino, L. Muccioli, J. Cornil, D. Beljonne, *Phys. Chem. Chem. Phys.* **2014**, *16*, 20279.
[21] G. D'Avino, S. Mothy, L. Muccioli, C. Zannoni, L. Wang, J. Cornil, D. Beljonne, F. Castet, *J. Phys. Chem. C* **2013**, *117*, 12981.
[22] A. Rao, P. C. Y. Chow, S. Gélinas, C. W. Schlenker, C.-Z. Li, H.-L. Yip, A. K. -Y. Jen, D. S. Ginger, R. H. Friend, *Nature* **2014**, *500*, 435.
[23] C. M. Proctor, M. Kuik, T.-Q. Nguyen, *Prog. Polym. Sci.* **2013**, *38*, 1941.
[24] G. Li, V. Shrotriya, J. Huang, Y. Yao, T. Moriarty, K. Emery, Y. Yang, *Nat. Mater.* **2005**, *4*, 864.
[25] F. C. Jamieson, E. B. Domingo, T. McCarthy–Ward, M. Heeney, N. Stingelin, J. R. Durrant, *Chem. Sci.* **2012**, *3*, 485.
[26] H. Uoyama, K. Goushi, K. Shizu, H. Nomura, C. Adachi, *Nature* **2012**, *492*, 234.
[27] B. Hu, L. Yan, M. Shao, *Adv. Mater.* **2009**, *21*, 1500.
[28] S. Wang, M. Kappl, I. Liebewirth, M. Müller, K. Kirchhoff, W. Pisula, K. Müllen, *Adv. Mater.* **2012**, *24*, 417.
[29] H. N. Tsao, D. M. Cho, I. Park, M. R. Hansen, A. Mavrinskiy, D. Y. Yoon, R. Graf, W. Pisula, H. W. Spiess, K. Müllen, *J. Am. Chem. Soc.* **2011**, *133*, 2605.
[30] G. Lakhwani, A. Rao, R. H. Friend, *Annu. Rev. Phys. Chem.* **2014**, *65*, 557.
[31] M. Parac, S. Grimme, *Chem. Phys.* **2003**, *292*, 11.
[32] A. Dreuw, M. Head-Gordon, *J. Am. Chem. Soc.* **2004**, *126*, 4007.
[33] N. Kuritz, T. Stein, R. Baer, L. Kronik, *J. Chem. Theory Comput.* **2011**, *7*, 2408.
[34] B. Baumeier , M. Rohlfing, D. Andrienko, *J. Chem. Theory Comput.* **2014**, *10*, 3104.
[35] T. B. de Quieroz, S. Kümmel, *J. Chem. Phys.* **2014**, *141*, 084303.
[36] G. Onida, L. Reining, A. Rubio, *Rev. Mod. Phys.* **2002**, *74*, 601.
[37] C. Faber, P. Boulanger, I. Duchemin, C. Attaccalite, X. Blase, *J. Chem. Phys.* **2013**, *139*, 194308.
[38] X. Blase, C. Attaccalite, *Appl. Phys. Lett.* **2011**, *99*, 171909.
[39] C. Faber, I. Duchemin, T. Deutsch, X. Blase, *Phys. Rev. B* **2012**, *86*, 155315.
[40] B. Baumeier, D. Adrienko, M. Rohlfing, *J. Chem. Theory Comput.* **2012**, *8*, 2790.
[41] O. A. Vydrov, G. E. Scuseria, *J. Chem. Phys.* **2006**, *125*, 234109.
[42] L. Kronik, T. Stein, S. Refaely Abramson, R. Baer, *J. Chem. Theory Comput.* **2012**, *8*, 1515.
[43] T. Stein, L. Kronik, R. Baer, *J. Am. Chem. Soc.* **2009**, *131*, 2818.
[44] A. Karolewski, T. Stein, R. Baer, S. Kümmel, *J. Chem. Phys.* **2011**, *134*, 151101.
[45] D. Di Nuzzo, A. Aguirre, M. Shahid, V. S. Gevaerts, S. C. J. Meskers, R. A. J. Janssen, *Adv. Mater.* **2010**, *22*, 4321.
[46] F. Provencher, M. Sakowicz, C.-N. Brosseau, G. Latini, S. Beaupré, M. Leclerc, L. X. Reynolds, S. A. Haque, R. Leonelli, C. Silva, *J. Polym. Sci. B: Polym. Phys.* **2012**, *50*, 1395.